



ΦΑΡΜΑΚΕΥΤΙΚΗ, 37, III, 2025 | 203-216

ΕΡΕΥΝΗΤΙΚΗ ΕΡΓΑΣΙΑ

PHARMAKEFTIKI, 37, III, 2025 | 203-216

RESEARCH ARTICLE

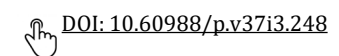
ZnO Nanoparticles Prepared by Hydrothermal Method and their Role on Gene Expression of TA System Type II Genes in Carbapenem-resistant Klebsiella pneumoniae

Saad H. Abood^{1,2}, Waad M. Raoof², Mohammed F. Al-Marjani³

¹College of Education, Al-Iraqia University, Baghdad, Iraq.

²College of Science, Tikrit University, Tikrit, Iraq.

³College of Science, Mustansiriyah University Baghdad, Iraq.



KEYWORDS: ZnO nanoparticle; Hydrothermal method; Carbapenem; K. pneumonia

Type II TA system.

ARTICLE INFO:

Received: January 4, 2025 Revised April 3, 2025 Accepted: May 14, 2025 Available on line: October 1, 2025

ABSTRACT

ZnO nanoparticles exhibit significant antibacterial activity against numerous pathogenic organisms in vitro and in vivo via penetration through the outer bacterial membrane leading to cytotoxicity or the generation of reactive oxygen species. This study examines the effects of hydrothermally produced ZnO nanoparticles on genes involved in toxin-antitoxin systems and the use of nanoparticles as antibiofilm in carbapenem-resistant *Klebsiella pneumoniae*. The result of the antibiotics sensitivity showed variable activity against K. pneumoniae, the isolates showed high resistance to carbapenem antibiotics including Imipenem (84%), and Meropenem (62%). The outcome demonstrated that ZnO nanoparticles have a 68% inhibitory effect on biofilm development. Using the microtiter plate method, the MIC concentration of ZnO nanoparticles as antibacterials was 19.5µg/ml. Several techniques were used to characterize ZnONPs: X-ray Diffraction Analysis (XRD), UV-visible spectroscopy, and Field emission scanning Electron microscopic (FESEM). The study's real-time PCR findings showed that after being treated with ZnO nanoparticles, the expression levels of the type II toxin-antitoxin genes (mqsR, mqsA, mazE, mazF, relE,relB, and *hipB*) had decreased.

Introduction

* CORRESPONDING AUTHOR: saad.h.abood@aliraqia.edu.iq

Antimicrobial resistance has become a global concern, emphasiz-

ing the urgent need for novel and effective antimicrobial strategies¹. Zinc oxide nanoparticles (ZnONP) have emerged as a promising an-

timicrobial agent due to their unique properties and ability to induce oxidative stress in bacterial cells^{2,3}. The present study investigates the potential of ZnONP in targeting toxin-antitoxin gene systems in *Klebsiella pneumoniae*, a significant opportunistic pathogen known for its multidrug resistance. Recent studies have highlighted the antimicrobial properties of ZnONP, demonstrating their ability to disrupt cell membranes, alter permeability, and accumulate within the cytoplasm, ultimately leading to cell death⁴. The mechanism of action is thought to involve the generation of reactive oxygen species, which can irreversibly damage cellular components, including DNA, proteins, and lipids^{1,3}.

Additionally, ZnONP has been reported to exhibit broad-spectrum antibacterial activity against various Gram-positive and Gram-negative strains, including Klebsiella pneumoniae^{3,5}. Toxin-antitoxin gene systems are an important mechanism bacteria employ to survive under environmental stresses, including antimicrobial exposure. These systems consist of a stable toxin and an unstable antitoxin, which work in a delicate balance to regulate cellular processes. Disruption of this balance can lead to cell death, making toxin-antitoxin systems a promising target for novel antimicrobial strategies. Bacterial chromosomes and plasmids contain a genetic component called the toxin-antitoxin system (TA). It comprises two genes that produce a labile antitoxin that counteracts the stable toxin⁶. According to antitoxin characteristics and mechanisms, TA systems have been divided into numerous kinds; type II TA systems are the most common⁷.

Usually, the antitoxin binds directly to the toxin and prevents it from doing its job by interfering with essential cellular processes such as transcription, translation, and DNA replication. In addition to being released when the antitoxins are broken down by cellular proteases under stress, the development of biofilm antibiotic tolerance, persistence, plasmid maintenance, phage resistance, and phage infectivity can also contribute to microbial pathogenicity⁸.

The transfer of genetic elements that serve as carriers of bacterial antibiotic resistance and virulence factors has often been associated with TA systems⁹.

The toxin and antitoxin in type II bacteria are proteins. Of all the bacterial TAs, type II TAs have been investigated the most, and many of them are found in different bacterial species, including the same species. According to the homology of the amino sequence of toxins, bacterial type II TA modules can be divided into 12 subgroups¹⁰. These include mqsRA¹¹, relEB¹², yefM-yoeB¹³, ω - ε - ζ ¹⁴, mazEF¹⁵, and yefM-yoeB¹³. In type II systems, the toxin acts as an inhibitor of essential cellular functions such as replication or protein synthesis. The primary causes of bacterial resistance in Iraq have been identified as public misconception and misuse of antibiotics¹⁶.

There is a significant rate of antibiotic misuse among the Iraqi population, ranging from 45% to 92%¹⁷. The spread of antibiotic-resistance genes from ambient bacteria to medically significant bacterial isolates is mostly facilitated by Klebsiella pneumoniae. Compared to the majority of bacterial isolates, K. pneumoniae is a rapidly developing MDR isolate that has been shown to develop antibiotic resistance at a faster rate. This is often a major worry for patients due to the increased risk of morbidity and mortality¹⁸. According to Mohammed et al. (2020) ¹⁹, a significant portion of *K. pneumoniae* exhibited considerable resistance to carbapenems, aminoglycosides, and ßlactam antibiotics. Recent research has shown that hvKp isolates have carbapenem resistance²⁰.

Zinc oxide (ZnO) nanoparticles (NPs) have gained significant attention due to their unique optical, electrical, and antimicrobial properties21. However, they also have several limitations that restrict their applications, including cytotoxicity, ZnO NPs can be toxic to human cells, especially at high concentrations, leading to potential health risks²². Overuse in antimicrobial applications may contribute to bacterial resistance²³. ZnO NPs tend to agglomerate due to high surface energy, reducing their effectiveness in applications like catalysis and drug delivery²¹ .They dissolve in acidic environments, limiting their use in certain biomedical or environmental applications. Under UV light, ZnO NPs can undergo photocorrosion, reducing their photocatalytic efficiency over time²³. Controlling size, shape, and surface properties consistently is difficult²⁴. Accumulation in or-

Activity	Primer target	Oligo Sequence 5'→3'	Product size(bp)	
HkG ²⁹	rpoB F: 5'-GTTGGCGAAATGGCGGAAAAC-3' R: 5'-ACGTCCATGTAGTCAACCTGG-3'		599	
TAs ³⁰	mqsR	F: 5'-ACGCACACCACATACACGTT-3' R: 5'-GCCTGGGTCTGTAAACATCCT-3'	194	
TAs ³⁰	mqsA	F: 5'-AATGTCCGGTTTGCCACCAG-3' R: 5'-GCATTCACCGAAGCCCGAAA-3'	238	
TAs ^{31,32}	mazE	F: 5'-ATGATCCACAGTAGCGTAAAGCGT-3' R: 5'-TTACCAGACTTCCTTATCTTTCGG-3'	249	
TAs ^{31,32}	mazF	F: 5'-ATGGTAAGCCGATACGTACCC-3' R: 5'-TGGGGCAACTGTTCCTTT-3'	288	
TAs ^{31,32}	relE	F: 5-'GACGAGCGGGCACTAAAGGAAT-3' R: 5'-TCAGAGAATGCGTTTGACCG-3'	267	
TAs ^{31,32}	relB	F: 5'-ATGGGTAGCATTAACCTGCGT-3' R: 5'-TCAGAGTTCATCCAGCGT-3	240	
TAs ^{31,32}	hipA	F: 5'-AGCCCAACGCAATTGGCGAATGCA-3' R: 5'- CTGTTCTGTTGATTCTGGCGAGGC-3'	1314	
TAs ^{31,32}	hipB	F: 5'AGCCCAACGCAATTGGCGAATG3' R: 5'-CTGTTCTGTTGATTCTGGCGAGGC-3'	225	

Table 1. Primers were used throughout the current study.

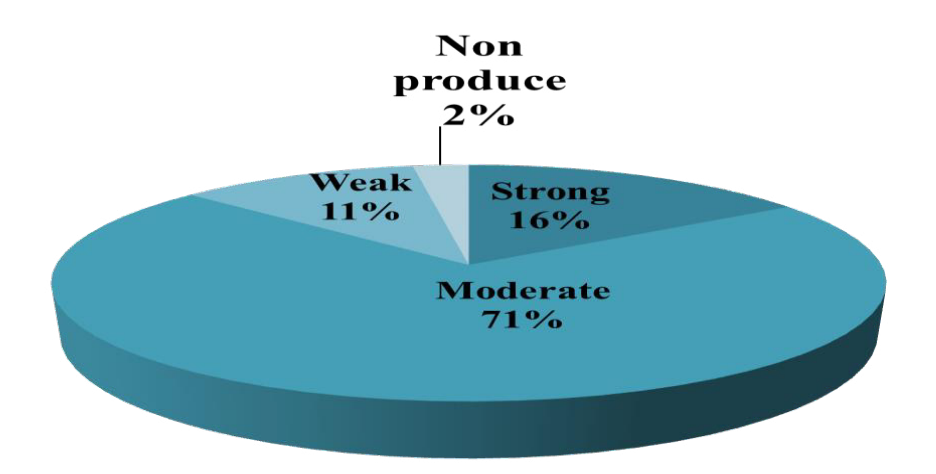
gans (e.g., liver, spleen) may cause long-term toxicity. Interactions with biological molecules (e.g., proteins, DNA) can lead to unintended side effects²¹. Alternatives like TiO₂, Ag, and SiO₂ NPs may offer better stability, lower toxicity, or enhanced performance in some applications²⁵.

The synthesis of enzymes like carbapenemases, AmpC β-lactamases, and extended-spectrum β lactamases (ESBLs)²⁶ or alterations in the outer membrane protein, permeability barrier, or target site represented by penicillin-binding protein are the main causes of *K. pneumoniae* antibiotic resistance, including beta-lactam antibiotics, which are one of the most important issues of elevated infection in hospitals²⁷. Multi-drug resistance (MDR) *K. pneumoniae* was thought to be treated with carbapenemases as a last resort. This occurred before *K. pneumoniae* initial description. Since the development of carbapenemase (KPC) in North Carolina isolates, carbapenem-resistant *K. pneumoniae* (Ckp) has been regularly found in a variety of nosocomial situations

worldwide. All β lactams and frequently other significant therapeutic drugs are ineffective against Ckp pathogens²⁸. The present study aims to investigate the efficacy of ZnO nanoparticles in targeting toxin-antitoxin gene systems in *Klebsiella pneumoniae*, to develop a novel and effective approach to combat antimicrobial resistance in this clinically significant pathogen.

Materials and Methods

Collection and identification of bacterial isolates: A total of 120 clinical isolates were collected and re-identified using selective media, biochemical tests, and the VITEK2 system (Bio-Merieux, France). The suspected isolates were collected over five months (from Dec 2023. to Oct. 2024) from different sources; urine samples, blood samples, sputum, burns, and wound swabs from several hospitals in Baghdad, including Al-Kindi Hospital, Baghdad Teaching Hospital, Al-Yarmouk Hospital (Iraq).



Biofilm formation

Figure 1. The total number of K. pneumoniae biofilm formation.

Detection of biofilm formation: In accordance with the protocol described by Kowalska et al. (2020) ²⁹, the microtiter plate method was used to assess biofilm formation.

ELISA: Using an ELISA reader, the absorbance of each well was determined at 630 nm. The control well's OD value was subtracted. The adherence capabilities of the bacterial test isolates were categorized into four groups based on all test OD values; the isolates were categorized using method described by Babapour et al. (2016) 30, with the mean optical density of the negative control (contained broth only) serving as the cut-off optical density (ODc).

Antibiotic susceptibility test: The disc diffusion method, as outlined by Salih et al. (2024)³¹, was implemented for the assessment of antibiotic susceptibility of *K. pneumoniae* isolates to various antibiotics.

Preparation of zinc oxide (ZnO): All row materials were analytical grade, ZnO nanostructure was synthesized using a simple hydrothermal method without catalysts, (0.05M) of hexahedral zinc nitrates $\text{Zn(NO}_3)_2.6\text{H}_2\text{O}$ (Scharlab, Spain) and (0.05 M) of HexaMethelTetramine (HMT) (Hi-media, India)

were dissolved in 80 ml of deionized water, the aqua solution was stirred for ten minutes. The aqua solution was transferred into a glass autoclave and kept at 90°C for 3 hours in a box furnace. After that, the autoclave cooled down to room temperature. The obtained powder was washed several times in ethanol, and distilled water, and dried. The hydrothermal conditions promote the growth of well-defined ZnO nanostructures. After autoclaving the collected white precipitate is ZnO nanoparticles. Dry the purified ZnO nanoparticles in an oven at 60–80°C to remove residual moisture.

Antibacterial activity of ZnO nanoparticle: Two methods were used to detect the effects of these nanomaterials on the inhibition or eradication of the cells of CKP isolates.

- (A) Microtiter Plate Method: By Jasim et al. (2020) ³², the MIC of nanomaterials was ascertained using single 96-well microdilution plates.
- (B) Well Diffusion Method: According to Yaseen et al. (2019)³³, the agar well diffusion method was used to screen for the antibacterial impact of nanomaterials.

Primer's: The effect of ZnO NPs against TA expression for genes (*mqsR*, *mqsA*, *mazE*, *mazF*, *relE*,*relB*,

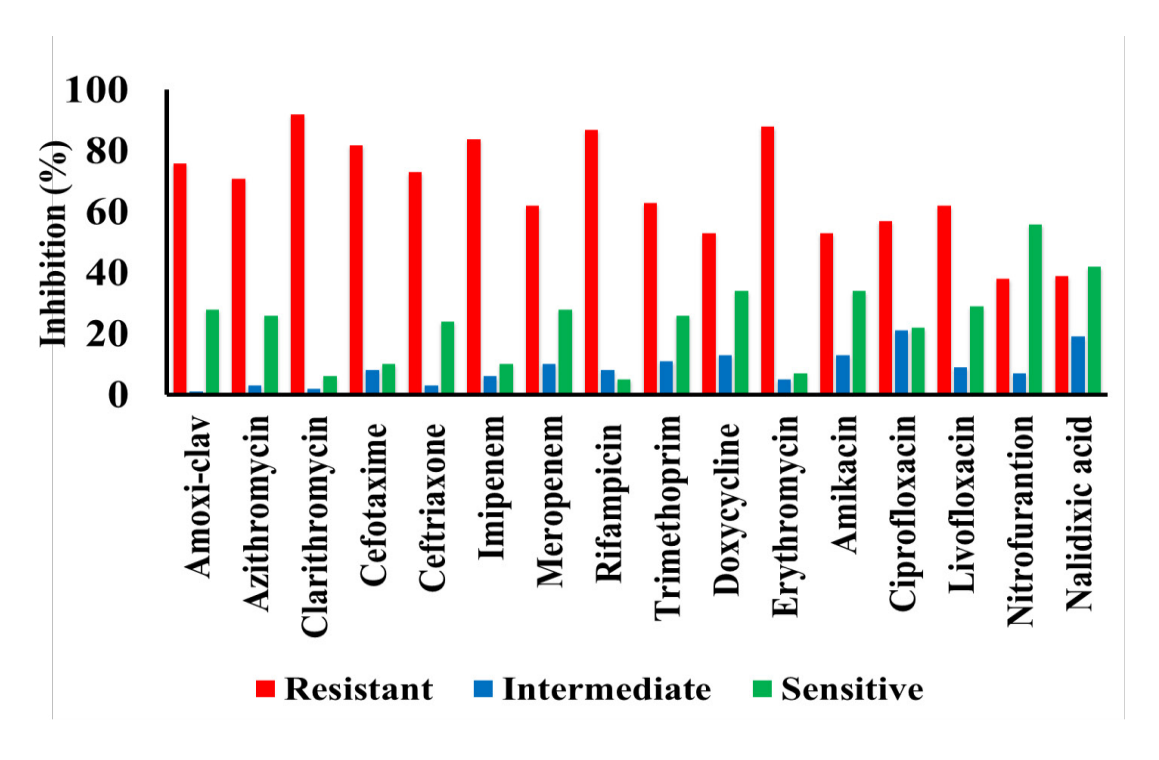


Figure 2. The percentage of antibiotic-resistant K. pneumoniae isolates.

and hipB) which is clarified in (Table 1)

Preparation of the selected isolates for RNA extraction: Three Carbapenem-resistant *K. pneumoniae* isolates with high antibiotic resistance and strong biofilm formation were chosen, and then *mqsRA,mazEF,relEB*, and *hipB* were selected. RT-qP-CR techniques were done before and after being treated with (ZnO) nanoparticles. The selective isolates were grown in BHI broth (Himedia, India) tubes overnight, then treated with a sub-mic concentration of nanoparticles for 4hr, and then RNA was extracted from isolates³⁴⁻³⁶.

Quantitative reverse transcription-PCR (qRT-PCR) assays: WizPureTM qPCR master (SYBR) (Wizbiosolution/South Korea) states that the qRT-PCR setup for each sample was as follows: cDNA served as the template, two reactions were carried out for each pair of primers, and the housekeeping rpoB gene was targeted as an internal control to normalize mRNA levels. Using 2^{Λ} - $\Delta\Delta$ CT, fold changes in mRNA expression were computed. For two hours, this reaction was

conducted in the Real Time-PCR system LM 2012. To avoid contamination, every stage of the qRT-PCR procedure was completed in a safety cabinet^{37,38}.

Results

Identification of *K. pneumoniae***:** The suspicious isolates were identified using selective media such as MacConkey agar, EMB agar, and Crhromo agar, biochemical assays, and the VITEK2 system.

Biofilm formation: The microtiter plate assay was done to determine the biofilm formation by *K. pneumoniae* isolates. The results showed that (117/120) isolates could produce biofilm, including (13/120) weak, (85/120) moderate, and (19/120) strong-biofilm producing isolates, while (3/120) isolates were non-biofilm producers as in (Figure 1).

Antibiotic susceptibility test: The result of the antibiotics sensitivity test for (16) antibiotics showed variable activity against *K. pneumoniae*,

PHARMAKEFTIKI, 37, III, 2025 | 203-216

RESEARCH ARTICLE

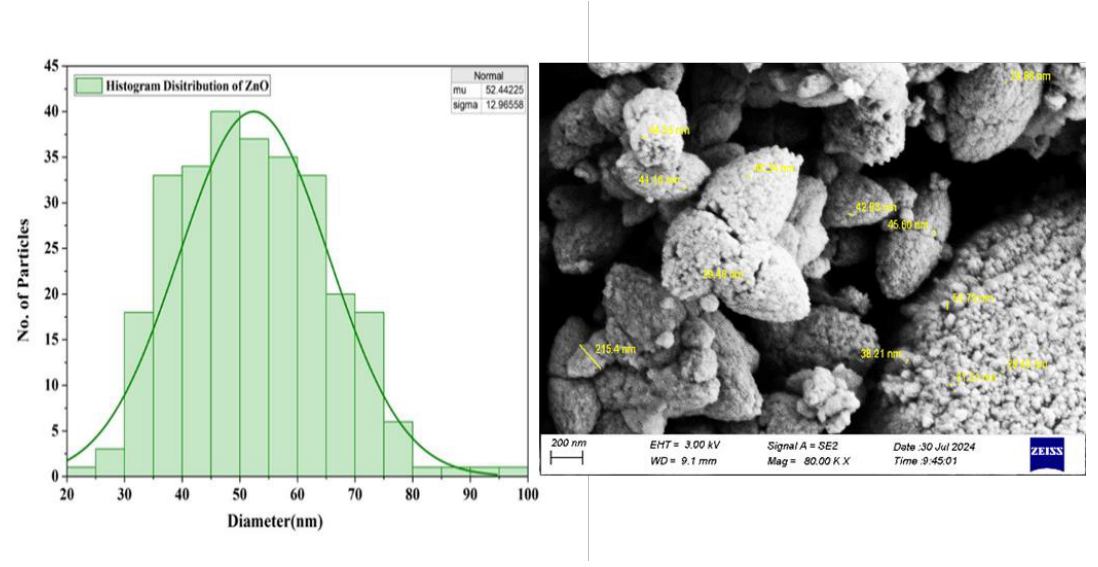


Figure 3. FE-SEM images of ZnO NPs as prepared by a hydrothermal method (Left image) histogram shows size distributions based on FE-SEM images of ZnO NPs (Right image) with scale bar 200 nm.

the isolates showed high resistance to carbapenem antibiotics including Imipenem (84%), Meropenem (62%), the resistant level of other antibiotics against *K. pneumoniae* were Clarithromycin (92%), Erythromycin (88%), Rifampicin (87%), Cefotaxime (82%), Amoxiclav (76%), Azithromycin (71%), Trimethoprim (63%), Levofloxacin (62%), Ciprofloxacin (57%), Doxycycline(53%), Amikacin (53%), Nalidixic acid (39%), Nitrofurantoin (38%) (Figure 2).

Characterization of ZnO nanoparticle

FE-SEM Images of ZnO: The result in (Figure 3) shows the FE-SEM analysis images of high-density ZnO NPs prepared using a hydrothermal method with different magnifications. Image (Left), obtained using ImageJ software of at least 45 particles, shows the particles have an average diameter of 52.44 nm. The minimum diameter of ZnO particles was 24.88 nm, and the maximum was 71.79 nm. Image (Right) shows that the product mainly consists of nanoparticles assembled to a spherical shape with found aggregation of nanoparticles with different diameters.

X-ray diffraction of ZnO: The result shows the XRD patterns of ZnO nanopowder prepared by the hydrothermal method. The diffraction peaks confirm the polycrystalline structure of ZnO with the Hexagonal phase. The observed peaks match well with the reported (JCPDS 96-900-4180) data of ZnO. All diffraction peaks in the XRD patterns correspond to the (100), (002), (101), (102), (110), (103), (200), (112), (201), (004) and (202) Miller indices. The higher peak intensities of an XRD pattern are due to the high crystallinity. The XRD patterns revealed that the (101) peak intensities were sharper and higher than others, implying that the growth orientation preferred the (101) peak as in (Figure 4). Diffraction patterns from zinc metal and impurities were not observed, indicating the high purity of the as-grown sample. The average crystallite size (D) of ZnO NPs is 27.87 nm.

UV- visible of ZnO: Adopts Visible-UV Spectroscopy enables the transmission of visible light and/or transmission of ultraviolet rays during the sample to determine the presence and/or amount of a substance that absorbs light inside the sample. UV vis-spectra detected the presence of ZnO nanopar-

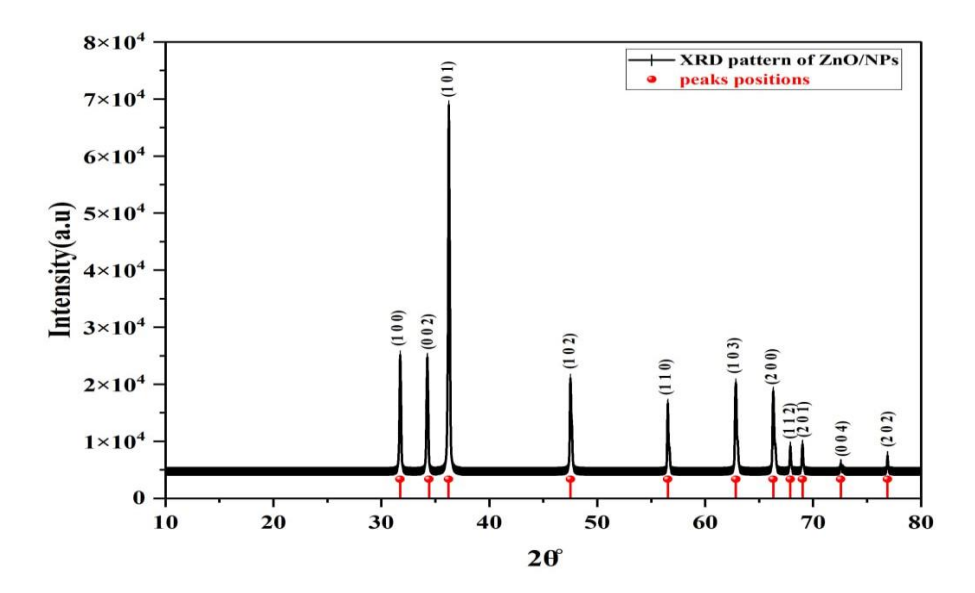


Figure 4. XRD pattern of as-prepared ZnO NPs by hydrothermal method.

ticles. The absorbance peak was reported at 366.65 nm as in (Figure 5).

Effect of ZnO NPs as Antibacterial: The result of using ZnO nanoparticles as an antibacterial against $\it K. pneumoniae$ by using microtiter plate assay using rezasurine pigment showed that MIC of ZnO was (19.5 µg/ml) as in (Figure 6A). Also, the inhibitory effect of ZnO NPs by the wells method showed good results as antibacterial the range size of the inhibition zone was (25 mm) as in (Figure 6B).

Effect of ZnO NPs as Antibiofilm: To investigate the inhibitory effects of (ZnO) nanoparticles on biofilm formation, we have chosen 19 strong biofilm *K. pneumoniae* isolates. The result showed that the inhibitory effects of (ZnO) nanoparticles as antibiofilm by microtiter plate assay were 68% positive and 32% negative as in (Figure 7).

Estimation of the effect of sub-MIC ZnO type II toxin-antitoxin system gene expression: The study's findings showed that after being treated with

ZnO nanoparticles, the expression levels of the type II toxin-antitoxin genes (*mqsR*, *mqsA*, *mazE*, *mazF*, *relE*,*relB*, and *hipB*) had decreased. as shown in (Table 2, Figure 8).

Discussion

In recent years, there has been a concerning rise in the prevalence of carbapenem-resistant *K. pneumoniae*, which poses a major threat to patient care due to the limited treatment options³⁹. One crucial factor contributing to the success of these multidrug-resistant strains is their ability to form robust biofilms, which can enhance their virulence, antibiotic tolerance, and persistence in the clinical setting⁴⁰. One study explored the impact of biofilm formation on the pathogenicity of carbapenem-resistant *K. pneumoniae*, particularly in the context of COVID-19 patients in intensive care units. The researchers found that these bacteria can cause severe infections, such as urinary tract infections, respiratory infections, and sepsis, in immunocompromised individuals⁴¹.

Carbapenem-resistant Enterobacteriaceae, includ-

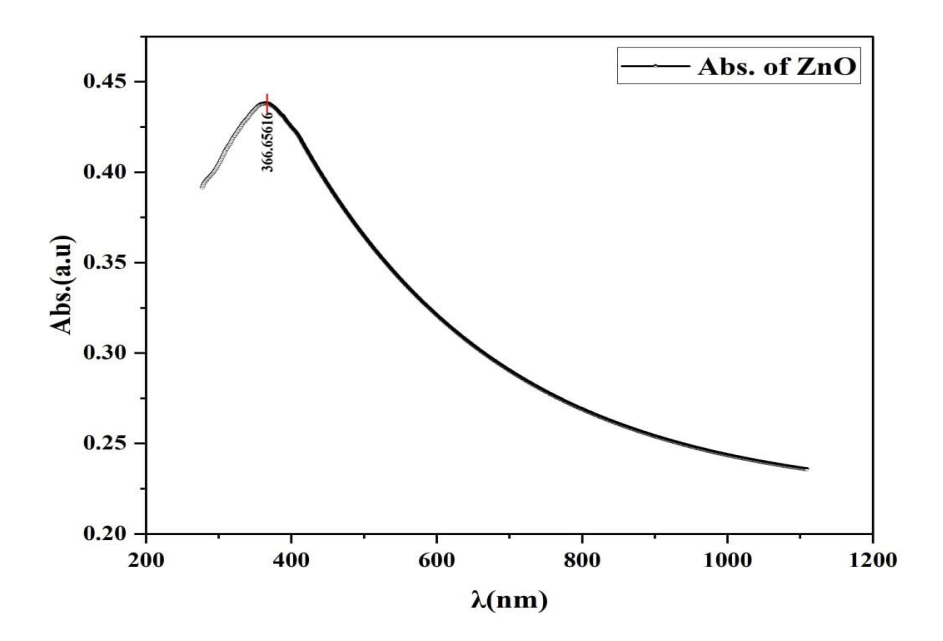


Figure 5. The UV-Vis spectrum of synthesized ZnO NPs by hydrothermal.

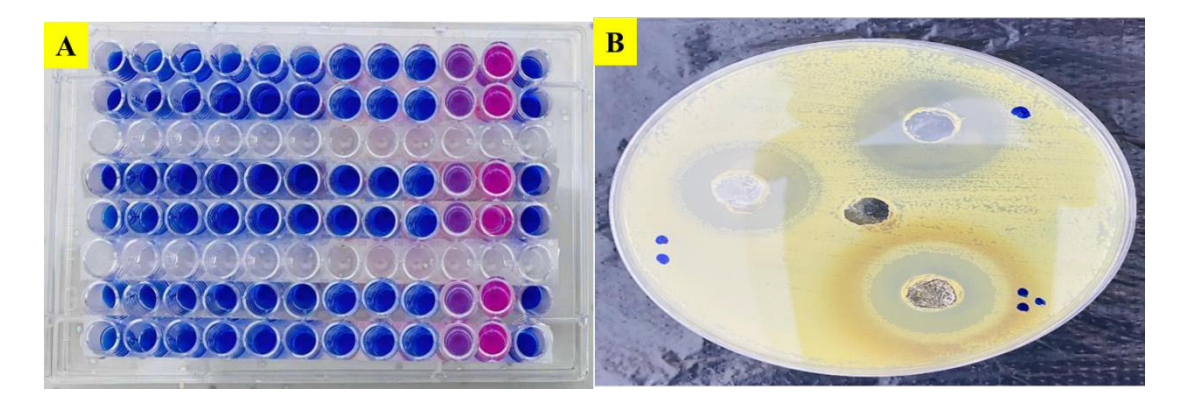


Figure 6. A-Determination of MIC of nanoparticles (ZnO) by Micro titer dilution method. B- Effect of nanoparticles against K. pneumoniae by well diffusion method.

ing carbapenemase-producing *K. pneumoniae*, have been responsible for nosocomial outbreaks globally and have become endemic in several countries⁴². These organisms possess potent resistance mechanisms that render them resistant to most, if not all, available antibiotic treatments, including the once "last line of defence" carbapenems and polymixins³⁹. The rapid spread and high mortality associated with

these infections have led to substantial morbidity, mortality, and healthcare costs, with estimates suggesting attributable mortality as high as 44%, particularly in the setting of bacteremia⁴².

The results of the study conducted by Mahmoud (2020) showed that ZnO nanoparticles prepared by green synthesis examined by (FE-SEM) have a range size diameter between (29-55 nm), and

Saad H. Abood et al., Pharmakeftiki, 37, III, 2025 | 203-216

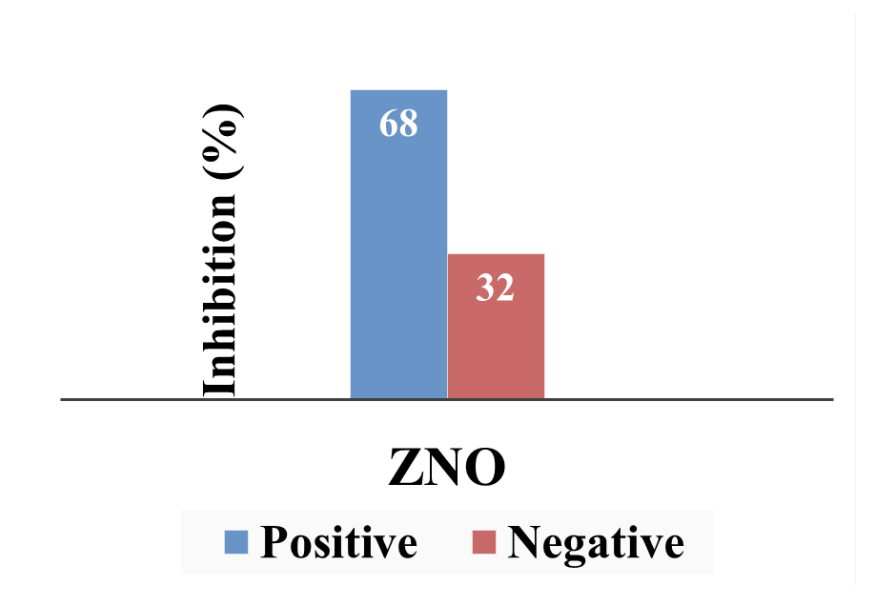


Figure 7. The effect of ZnO nanoparticle as antibiofilm against K. pneumoniae.

Table 2. CT, Δ CT values, fold change (2- Δ Δ CT), and log2 fold change of type II toxin-antitoxin system genes (relE,relB, mqsR,mqsA, mazE,mazF, hipB) after sub-MIC ZnO treatments.

		Ct		ΔCt		ΔΔCt	Fold change	Log 2 -
Colour of	Genes	before treatment	after treatment ZnO	before treatment	after treatment ZnO	after treatment ZnO		
	mqs R	22.9	30.44	0.78	7.32	6.54	0.0107	-1.9687
	mqs A	22.89	31.57	-0.23	8.45	8.68	0.0024	-2.612
	maz E	22.98	32.60	-0.14	9.48	9.62	0.0012	-2.8959
	maz F	23.17	32.98	0.05	9.86	9.81	0.0011	-2.9531
	relE	23.2	32.14	0.08	9.02	8.94	0.0020	-2.6912
	relB	23.54	34.00	0.42	10.88	10.46	0.0007	-3.1487
	hipB	23.25	31.86	0.13	8.74	8.61	0.0025	-2.5918

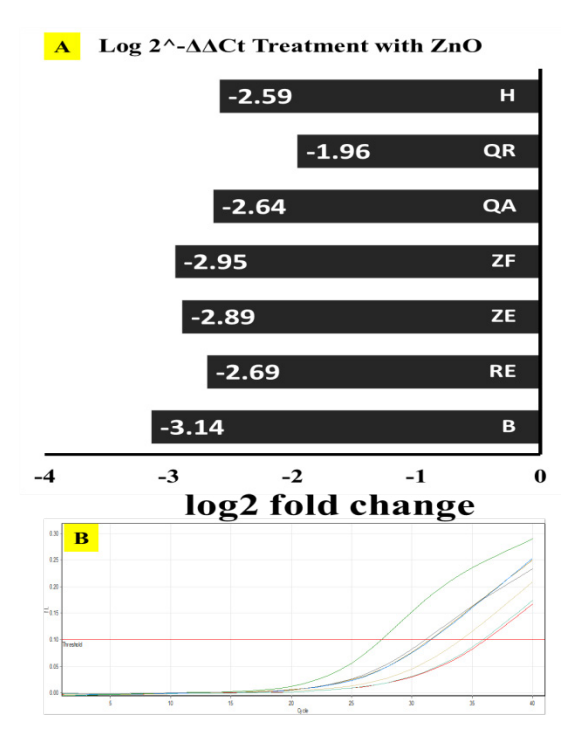


Figure 8. (A) log2 fold change gene expression of type II toxin-antitoxin system genes (relE, relB, mqsR,mqsA, mazE,mazF, hipB) after sub-MIC ZnO treatments. (B) Standard curve RT-PCR amplification of TAs genes plot by qRT-PCR. The colours represented the different TAs genes of K. pneumoniae after sub-MIC ZnO treatments.

the nanoparticles were irregular or polymorphic shapes³⁸. A local study shows that the ZnO prepared by the hydrothermal method has a pure wurtze hexagonal structure as compared with (JCPDS) cards44. Also, no peaks of metallic Zn are observed Which means that the O2 ratio in the gas mixture is sufficient for the complete oxidation of Zn independently and no additional thermal annealing in the oxidation atmosphere is needed, also no other peaks appear for the organic material used in a paste made. The highly blue-shifted maximum absorption occurring at about 366.65 nm confirms the formation of the nanoscale ZnO component since the maximum absorption for the bulk ZnO occurs at around 385 nm⁴⁵. The unique physicochemical properties of ZnO nanoparticles, including their high surface-to-volume ratio and reactive oxygen species generation, have been identified as key factors contributing to their antibacterial efficacy. Nu-

merous studies have demonstrated the potent antibacterial activity of ZnO nanoparticles against both Gram-positive and Gram-negative bacteria⁴⁶. The proposed mechanisms of action include disruption of the bacterial cell membrane, interference with cellular processes, and generation of oxidative stress leading to cell death⁴⁷. The findings indicated that isolates with significant biofilm formation were highly prevalent in wound and UTI infections. Using catheters and the necrotic tissue of wounds serve as a substrate for bacterial attachment, which may be the cause⁴⁷. Furthermore, the MDR isolates developed biofilms at a significantly higher rate. The findings were consistent with a local investigation by Abdelraheem and Mohamed (2021), that found that isolates from wound and burn swabs that produced biofilms had more antibiotic resistance than those that did not 48. According to the study conducted by Hassan (2024) findings, temperature (30°C, 37°C, and 44°C) and pH (5, 7, 9, and 11) had a substantial differential impact on the gene expression levels of hipB anti-toxin, mqsR toxin, and relE toxin⁴⁹. The activity of enzymes, which are essential for gene expression and other cellular functions, can be affected by temperature and pH. These factors can trigger the SOS stress response and alarmone (p)ppGpp, which controls genes like TA system genes or enzymes for growth and stress survival⁵⁰. The mqsRA TA system has been shown in recent studies to exhibit reduced expression of the mqsA antitoxin under stress⁵¹. And increased expression of the *mqsR* gene, which indicates a 3.67-fold rise in the *relE* gene⁵².

References

- 1. Mohana S., Sumathi S. Synthesis of zinc oxide using Agaricus bisporus and its in-vitro biological activities. *J. Environ. Chem. Eng.* 8(5), 104192, 1-8, 2020.
- 2. Khaleel L.W., Abdulhamed A.A. Antidiabetic effect of Glycyrrhizin glabra extract and Glycyrrhiza glabra Silver nanoparticle in female rats. Pharmakeftiki. 36(3), 67-82, 2024.
- Hamad A.M., Atiyea Q.M., Hameed D.N., Dalaf A.H. Green synthesis of copper nanoparticles using strawberry leaves and study of properties, anti-cancer action, and activity against bacteria isolated from Covid-19 patients. *Karbala Int. J. Mod. Sci.* 9(1), 1-17, 2023.
- 4. Kumar R., Umar A., Kumar G., Nalwa H.S. Antimicrobial properties of ZnO nanomaterials: A review. *Ceram. Int.* 43(5), 3940-61, 2017.
- Hamad A.M., Atiyea Q.M. Study the effect of zinc oxide nanoparticles and dianthus caryophyllus L. extract on streptococcus mutans isolated from human dental caries in vitro. *InAIP Conference Proceedings*. 2398(1), 1-10, 2022.
- 6. Bordes P., Genevaux P. Control of toxin-antitoxin systems by proteases in Mycobacterium tuberculosis. *Front. Mol. Biosci.* 8,691399, 1-10, 2021.
- 7. Wojciechowska M., Równicki M., Mieczkowski A.,

Conclusion

We investigate from the above that ZnO nanoparticles have activity against (Ckp) isolates in addition to having antibiofilm activity, it has also been proven that ZnO NPs affect gene expression of toxin-antitoxin type II, whether it increases or decreases depending on the type of targeted gene. This is considered a promising solution to eliminate the problem of bacterial resistance to antibiotics by disrupting the toxin-antitoxin system and allowing the toxin to kill bacteria or cause significant damage to them, it reduces their virulence and prevents them from being able to cause infection. \square

- Miszkiewicz J., Trylska J. Antibacterial peptide nucleic acids—facts and perspectives. *Molecules*. 25(3), 1-22, 2020.
- 8. Chattopadhyay D., Stevenson S., Broekgaarden F., Antonini F., Belczynski K. Modelling the formation of the first two neutron star–black hole mergers, GW200105 and GW200115: metallicity, chirp masses, and merger remnant spins. *Mon. Not. R. Astron. Soc.* 513(4), 5780-9, 2022
- Horesh G., Fino C., Harms A., Dorman M.J., Parts L., Gerdes K., Heinz E., Thomson N.R. Type II and type IV toxin–antitoxin systems show different evolutionary patterns in the global Klebsiella pneumoniae population. *Nucleic Acids Res.* 48(8), 4357-70, 2020.
- Leplae R., Geeraerts D., Hallez R., Guglielmini J., Dreze P., Van Melderen L. Diversity of bacterial type II toxin–antitoxin systems: a comprehensive search and functional analysis of novel families. *Nucleic Acids Res.* 39(13),5513-25, 2011.
- 11. Brown B.L., Grigoriu S., Kim Y., Arruda J.M., Davenport A., Wood T.K., Peti W., Page R. Three dimensional structure of the MqsR: MqsA complex: a novel TA pair comprised of a toxin homologous to RelE and an antitoxin with unique properties. *PLoS Pathogens*. 5(12), e1000706, 2009.
- 12. Takagi H., Kakuta Y., Okada T., Yao M., Tanaka I., Kimura M. Crystal structure of archaeal toxin-an-

- titoxin RelE–RelB complex with implications for toxin activity and antitoxin effects. *Nat. Struct. Mol. Biol.* 12(4), 327-31, 2005.
- 13. Kamada K., Hanaoka F. Conformational change in the catalytic site of the ribonuclease YoeB toxin by YefM antitoxin. *Mol. Cell.* 19(4), 497-509, 2005.
- 14. Zielenkiewicz U., Cegłowski P. The toxin-antitoxin system of the streptococcal plasmid pSM19035. *J. Bacteriol.* 187(17), 6094-105, 2005.
- Aizenman E., Engelberg-Kulka H., Glaser G. An Escherichia coli chromosomal" addiction module" regulated by guanosine [corrected] 3', 5'-bispyrophosphate: a model for programmed bacterial cell death. *Proc. Natl. Acad. Sci.* 93(12), 6059-63, 1996.
- 16. Al-Taie A., Hussein A.N., Albasry Z. A cross-sectional study of patients' practices, knowledge and attitudes of antibiotics among Iraqi population. *J. Infect. Dev. Ctries.* 15(12), 1845-53, 2021.
- 17. Salim K.S., Alsabah A.S., Taghi H.S. Misuse of antibiotics in Iraq: A review of Iraqi published studies. *Al-Mustansiriyah J. Sci.* 21(2), 15-20, 2021.
- Nirwati H., Sinanjung K., Fahrunissa F., Wijaya F., Napitupulu S., Hati V.P., Hakim M.S., Meliala A., Aman A.T., Nuryastuti T. Biofilm formation and antibiotic resistance of Klebsiella pneumoniae isolated from clinical samples in a tertiary care hospital, Klaten, Indonesia. *InBMC Proceedings*. 13, 1-8, 2019.
- Mohammed H.H., Saadi A.T., Yaseen N.A. detection of carbapenem antibiotic resistance in klebsiella pneumonia in Duhok city/Kurdistan region/Iraq. *Duhok Med. J.* 14(1), 28-43, 2020.
- 20. Zhao Q., Guo L., Wang L.F., Zhao Q., Shen D.X. Prevalence and characteristics of surgical site hypervirulent *Klebsiella pneumoniae* isolates. *J. Clin. Lab. Anal.* 34(9), e23364, 2020.
- Akshay K., Roy A., Snega R. Aspergillus flavus Mediated Extracellular One-pot Synthesis of Zirconium and Titanium Oxide Nanoparticles and their Antioxidant and Antiinflammatory Efficacy Study. *Texila Int. J. Public Health.* 13(1),145-154, 2025.
- 22. Gopalakrishnan K., Ramesh A., Devendran A., Palaniyandi S., Elumalai L., Loganathan K., Elumalai P., Anbazhagan G.K. Anti-biofilm Effects of Res-

- in-Modified Glass-Ionomers Incorporated with Silver Nanoparticles and Sodium Fluoride. *Texila Int. J. Public Health* 13(1), 179-187, 2025.
- 23. Sebastian S., Martin T.M., Kumar M.S.K. Nanoparticle-Driven Healing: Evaluating Chitosan-Copper in Zebrafish Wound Recovery. *Texila Int. J. Public Health* 13(1), 332-342, 2025.
- 24. Ryntathiang I., Chaudhary D.G., Pooja Y., .Behera A., Chandrasekaran Y., Jothinathan M.K.D. Ecofriendly Synthesis of Cobalt Nanoparticles Using Millettia pinnata and Evaluation of Embryonic Toxicology and Anticancer Activity. *Texila Int. J. Public Health* 13(1), 487-493, 2025.
- Dinesh G., Lakshmi T., Rajeshkumar S. Green Synthesis of Selenium Nanoparticles using Vaccinium Subg. Oxycoccus for Antioxidant, Anti-Inflammatory, and Cytotoxic Effect. *Texila Int. J. Public Health* 13(1), 645-659, 2025.
- 26. Ahmed B., Ameen F., Rizvi A., Ali K., Sonbol H., Zaidi A., Khan M.S., Musarrat J. Destruction of cell topography, morphology, membrane, inhibition of respiration, biofilm formation, and bioactive molecule production by nanoparticles of Ag, ZnO, CuO, TiO2, and Al2O3 toward beneficial soil bacteria. *ACS Omega*. 5(14), 7861-76, 2020.
- 27. Samanje J., Mohammed A.S., Al-Hamami M.S. Phenotypic and Genotypic Detection of Extended-spectrum β-lactamase production by Klebsiella pneumoniae Isolated from Different Clinical Samples in Baghdad, Iraq. *J. Pure Appl. Microbiol.* 15(3), 1681-8, 2021.
- 28. Annavajhala M.K., Gomez-Simmonds A., Uhlemann A.C. Multidrug-resistant Enterobacter cloacae complex emerging as a global, diversifying threat. *Front. Microbiol.* 10:44, 1-8, 2019.
- 29. Kowalska J., Maćkiw E., Stasiak M., Kucharek K., Postupolski J. Biofilm-forming ability of pathogenic bacteria isolated from retail food in Poland. *J. Food Prot.* 83(12), 2032-40, 2020.
- 30. Babapour E., Haddadi A., Mirnejad R., Angaji S.A., Amirmozafari N. Biofilm formation in clinical isolates of nosocomial Acinetobacter baumannii and its relationship with multidrug resistance. *Asian Pac. J. Trop. Biomed.* 6(6), 528-33, 2016.
- 31. Salih A.Y., Al-Taii H.A., Ismael N.S., Merkhan M.M.

- Inhibition of Biofilm Formation and Pyocyanin Production from Multidrug Resistance P. aeruginosa by Using Vitamin C, Salicylic Acid, and Multisera. *Texila Int. J. Public Health* 12(4), 1-12, 2024.
- 32. Jasim S.A., Abdulrazzaq S.A., Saleh R.O. Virulence Factors of Klebsiella pneumoniae Isolates from Iraqi Patients. *Sys. Rev. Pharm.* 11(6), 916-921, 2020
- 33. Yaseen S.M., Abid H.A., Kadhim A.A., Aboglida E.E. Antibacterial activity of palm heart extracts collected from Iraqi Phoenix dactylifera L. *J. Tech.* 1(1), 52-9, 2019.
- 34. Mahmood, I.M. Genotypic and Phenotypic Detection of Hypervirulent Klebsiella pneumoniae Isolated from Clinical Specimens in Baghdad Hospitals. *Thesis Mustansiriyah University*. 2022.
- 35. Al Husseini L.B., Maleki A., Al Marjani M.F. Antisense mqsR-PNA as a putative target to the eradication of Pseudomonas aeruginosa persisters. *New Microbes New Infect.* 41,100868, 2021.
- 36. Hemati S., Azizi-Jalilian F., Pakzad I., Taherikalani M., Maleki A., Karimi S., Monjezei A., Mahdavi Z., Fadavi M.R., Sayehmiri K., Sadeghifard N. The correlation between the presence of quorum sensing, toxin-antitoxin system genes and MIC values with ability of biofilm formation in clinical isolates of Pseudomonas aeruginosa. *Iran J. Microbiol.* 6(3), 133-139, 2014.
- 37. Karimi S., Ghafourian S., Kalani M.T., Jalilian F.A., Hemati S., Sadeghifard N. Association between toxin-antitoxin systems and biofilm formation. *Jundishapur J. Microbiol.* 8(1), e14540, 2014.
- 38. Khalid I, Nayyef NS, Merkhan MM. A Taxonomic Study comparing the two types of Medicinal Leeches available in Iraq. *Res. J. Pharm. Tech.* 15(3), 1119-22, 2022.
- 39. Arato V., Raso M.M., Gasperini G., Berlanda Scorza F., Micoli F. Prophylaxis and treatment against Klebsiella pneumoniae: current insights on this emerging anti-microbial resistant global threat. *Int. J. Mol. Sci.* 22(8), 4042, 1-20, 2021.
- 40. Wang G., Zhao G., Chao X., Xie L., Wang H. The characteristic of virulence, biofilm and antibiotic resistance of Klebsiella pneumoniae. *Int. J. Envi-*

- ron. Res. Public Health. 17(17), 6278, 2020
- Mędrzycka-Dąbrowska W., Lange S., Zorena K., Dąbrowski S., Ozga D., Tomaszek L. Carbapenem-resistant Klebsiella pneumoniae infections in ICU COVID-19 patients—A scoping review. J. Clin. Med. 10(10), 2067, 2021.
- 42. Rees C.A., Nasir M., Smolinska A., Lewis A.E., Kane K.R., Kossmann S.E., Sezer O., Zucchi P.C., Doi Y., Hirsch E.B., Hill J.E. Detection of high-risk carbapenem-resistant Klebsiella pneumoniae and Enterobacter cloacae isolates using volatile molecular profiles. Sci. Rep. 8(1), 13297, 2018.
- 43. Mahmoud A.H. Biosynthesis and characterization of some nanoparticles by using plant extracts and studying their antimicrobial property against pathogenic bacteria isolated from wounds and burns. *Thesis University of Diyala*. 2020.
- 44. Al-Khafaji O.A. Synthesis and studying characterization of ZnO nanostructures and its sensor Applications. *Thesis Mustansiriyah University*. 2015.
- Senthilkumar S.R., Sivakumar T. Green tea (Camellia sinensis) mediated synthesis of zinc oxide (ZnO) nanoparticles and studies on their antimicrobial activities. *Int. J. Pharm. Pharm. Sci.* 6(6), 461-5, 2014.
- Renjusha S., Vaisakh P.H. Green synthesis and characterization of ZnO nanoparticles from leaf extracts of Barrintonia acutangula and its antibacterial activity. *Rasayan J. Chem.* 14(3), 1653-8, 2021.
- 47. Jalil M.B., Al Atbee M.Y. The prevalence of multiple drug resistance Escherichia coli and Klebsiella pneumoniae isolated from patients with urinary tract infections. *J. Clin. Lab. Anal.* 36(9), e24619, 1-7, 2022.
- 48. Abdelraheem W.M., Mohamed E.S. The effect of Zinc Oxide nanoparticles on Pseudomonas aeruginosa biofilm formation and virulence genes expression. *J. Infect. Dev. Ctries.* 15(06), 826-32, 2021.
- 49. Hassan F.J. Influence of Temperature and pH Values on Klebsiella pneumoniae Toxin-Antitoxin Gene Expression. *Thesis Mustansiriyah University*. 2024.
- 50. Pacios O., Blasco L., Bleriot I., Fernandez-Garcia

PHARMAKEFTIKI, 37, III, 2025 | 203-216

RESEARCH ARTICLE

- L., Ambroa A., López M., Bou G., Cantón R., Garcia-Contreras R., Wood T.K., Tomás M. (p) ppGpp and its role in bacterial persistence: new challenges. *Antimicrob. Agents Chemother*. 64(10), 10-128, 2020.
- 51. Al Husseini L.B., Maleki A., Al Marjani M.F. Antisense mqsR-PNA as a putative target to the erad-
- ication of Pseudomonas aeruginosa persisters. *New Microbes New Infec.* 41,100868, 2021.
- 52. Narimisa N., Kalani B.S., Amraei F., Mohammadzadeh R., Mirkalantari S., Razavi S., Jazi F.M. Type II toxin/antitoxin system genes expression in persister cells of Klebsiella pneumoniae. *Rev. Res. Med. Microb.* 31(4), 215-20, 2020.